European purse seiners CPUE standardization of Big Eye tuna caught under dFADs.

Akia S[1.2]., Guery L[3]., Grande M[4]., Kaplan D[2]., Baéz J.C[5]., Ramos M. L[5]., Uranga J[4], Abascal F[5]., Santiago J[4], Merino G[4]., Gaertner D[2].

Summary

Abundance index for Big Eye tuna (BET) in the Indian Ocean was derived from the European purse seiner CPUEs series (2010-2021) for fishing operations made on drifting FADs (Fishing aggregating Devices). By classifying sets to non-followed dFADs (i.e., dFADs randomly encounter for which the purse seiner has no previous information) and followed-dFADs (dFADs from which purse seiner has previous information and therefore it is not randomly encounter) we take into account the difference between them. The VAST methodology was used to standardized the BET CPUE. A GLMM approach has been also applied to compare the outputs when using an alternative modelling approach

Keyword: Vector autoregressive spatio-temporal model (VAST), dFAD, Abundance index; CPUE standardization; Purse seiner; Big Eye tuna

[1] Corresponding author: sosthene.akia@ird.fr
[2] Institut de Recherche pour le Développement (IRD), UMR MARBEC, CS 30171, Av. JeanMonnet, 34203 Sete Cedex, France.
[3]Centre International de Recherche en Agronomie pour le Développement (CIRAD), UMR PHIM, Team PRISM – FORISK, TA A-120 / D Campus international de Baillarguet 34398 Montpellier Cedex 5 France.
[4]AZTI, Marine Research, Basque Research and Technology Alliance (BRTA). Txatxarramendi ugartea z/g, 48395 Sukarrieta - Bizkaia, Spain.
[5]Instituto Español de Oceanografía, Centro Oceanográfico de Málaga, Puerto Pesquero, s/n Apdo., 29640, Fuengirola, Málaga, Spain

1. Introduction

Interpreting changes over time in CPUE series as a trend in abundance has always been a major challenge for scientists working in stock assessment. In the case of the tropical tuna purse seiner fishery operating in the Indian Ocean, there are several factors affecting the CPUE-abundance relationship. One aspect of tropical tuna purse seine fisheries that has seen significant technological change over recent decades is fishing on fish schools associated with floating objects attached to instrumented buoys (FOBs) (ICCAT, 2016).

In this paper, we estimate standardized catch per unit effort (CPUE) time series for Big Eye tuna (BET) to be provided to the IOTC as an input for the upcoming BET stock assessment. CPUE time series were standardized for BET caught during fishing operations on drifting FADs by the the European purse seiner fleet. A catchability covariate, "Is_fishing_owned dFAD" (i.e. if fishing occurred in tracked dFADS) , has been introduced in the model to take into account the difference between fishing operations made on dFADs followed by the vessel (or vessel´s company) and fishing operations made on the other dFADs randomly encountered (coded True or False, respectively). Indeed, in the case of non-followed dFADs sets, the purse seiner (nor the company) has no previous information for detecting the object nor on the corresponding aggregated biomass.

The methodology for catched tuna schools associated to dFADs used in this paper is based on a spatio-temporal Delta generalized linear mixed models (GLMM) (Thorson, 2019). This model structure makes it possible to better take into account spatial and temporal variations and to better estimate the standard errors of the standardized CPUE.

2. Materials and methods

2.1 Conventional fishing data cleanning

To derive European purse seiner standardized CPUEs for the BET stock assessment, T3-processed logbook data from the French and Spanish purse seine fleets targeting tropical tunas in the Indian Ocean from 2010 to 2021 were analyzed. Raw logbook data (Level0) produced by the skippers were corrected in terms of total catch per set (to account for the difference between reported catch at sea and landed catch) and species composition (based on port size sampling and the T3 methodology – see (Pallarés and Hallier, 1997)) to generate the Level 1 logbook database used in this paper. The Exploited Tropical Pelagic Ecosystems Observatory (IRD-Ob7) and the Spanish Institute of Oceanography (IEO), respectively provided logbook data for the French and the Spanish fleets.

The analysis was restricted to:

- The period 2010-2021. Data for 2010-2021 are for both the European purse seiner fleets, excepted for 2020, covered only French fleets and for 2021 covered only Spanish fleets.
- Total number of sets per day per boat was filtered and days with unrealistic data (> 5 sets) were removed
- Entire days with at least one activity with problematic operations (e.g., equipment failures) were removed.
- High-seas and all EEZs except for the Somali EEZ due to the effects of piracy were selected (Okamoto, 2011; Chassot *et al.*, 2012; Guillotreau *et al.*, 2012).

- Only the area defined by all 5*5 degree grid cells where BET were fished for at least 274 sets (0.5%) over the study period were selected to avoid areas that are not routinely fished.

2.2 Sets classification

Sets to FADs were classified based on whether the vessel had access to buoy information prior to the set or not. On one side, for French dataset, the sets were classified according to the method presented in Wain et al. (2020). On the other hand, for Spanish dataset the following steps have been followed:

- The daily GPS positions of the buoys have been considered. One position per day was available including information of the latitude, longitude, speed and ownership of the buoys (a unique purse seine vessel and/or vessel´s company). To have the GPS position of buoys at water, those having erroneous location, buoys on land positions; and on-board buoy positions have been removed from the database following the methodology described in Grande et al. (2019).

- Daily buoy positions have been linearly interpolated to estimate hourly buoy positions.

- Buffer areas of 4 km have been established around each set.

- In order to discard new FAD deployments, buoys with GPS position at least two days prior to the set have been considered for set classification.

- Each set was classified according to the buoys´ ownership present in the buffer area the same day of the set or the day before. If a buoy of the vessel was present in the buffer area, the set was classified as a set made to an owned buoy, from which the vessel is supposed to have the information prior to setting. If a buoy belonging to the vessel was not present in the buffer area, but a buoy belonging to the company was present, the set was classified as made to a company´s buoy, from which the vessel could have the information prior to setting. The sets classified to be made to owned or corresponding company´s buoys were grouped as owned-sets. If the buoy in the buffer area did not belong to the vessel nor to the company, the set was classified as made to a non_owned (I.e.,non-followed) buoy, from which it is supposed that the vessel did not have the information prior to the set.

2.3 GLMM

A delta-GLMM was applied to standardize the CPUE time series for BET in Indian Ocean developed with the fishing operations made on drifting FADs. A stepwise regression was applied to each GLMM model component of the delta model with all the explanatory variables and interactions to determine those factors that significantly contributed to explain the deviance of the model. For this, deviance analysis tables was created. Final selection of explanatory factors was conditional to: a) the relative percentage of deviance explained by adding the factor in evaluation and b) The Chi-square ($\chi 2$) significance test. Those factors that explained less than 2% of the variability of the model were not considered.

Interactions of the temporal component (year-quarter) with the rest of the variables were also evaluated. If an interaction was statistically significant, it was then considered as a random

interaction(s) within the final model. The positive catch rate component was modeled with a lognormal error distribution. The most significant explanatory factors were incorporated in the following delta-GLMM (**Table 1, 2 and 3**).

Binomial component: y12 ~ yyqq +pays. (1)

Positive catch rate component: log(bet) ~ yyqq +area+(1|numbat)+(1|yyqq:area) (2)

where vessel (numbat) and the interaction quarter*area (yyqq:area) were incorporated as random effects.

2.4 GLMM into spatio-temporal model (VAST methodology)

Spatiotemporal models have been shown to be more accurate and less biased than equivalently structured delta-GLMs when fit to fisheries dependent data (Grüss *et al.*, 2019). The VAST spatiotemporal modeling approach (Thorson, 2019) was used to generate relative standardized CPUE time series for Big Eye tuna in the Indian Ocean to be provided to the IOTC as an input for the upcoming IOTC BET stock assessment. In the VAST spatiotemporal modeling approach, the standardized CPUE is the spatial average of predicted abundance once catchability effects have been « standardized" out. Additionally, the spatial abundance distributions predicted from the VAST model can be used to calculate the regional weighting factors for the assessment regions. The model implemented by the VAST package (version 3.9), a spatiotemporal delta generalized linear mixed model (GLMM), is an extension of the delta-GLMM described in the previous section. An interactive relationship between space and time, as opposed to an additive one, is specified using Gaussian random fields to define the spatial and spatiotemporal components of the model (Thorson *et al.*, 2015). These Gaussian random fields are defined with a Matern covariance function. We applied the VAST methodology to estimate the model described in the last section regarding the GLMM.

VAST potentially includes two linear predictors (because it is designed to support delta-models, which include two components). The first linear predictor $r_1(i)$ represents encounter probability in a delta-model, or zero-inflation in a count-data model:

$$p_1(i) = \underbrace{\beta_1(c_i, t_i)}_{\text{Temporal variation}} + \underbrace{\omega_1^*(s_i, c_i)}_{\text{Spatial variation}} + \underbrace{\varepsilon_1^*(s_i, c_i, t_i)}_{\text{Spatio-temporal variation}} + \underbrace{\eta_1(v_i, c_i)}_{\text{Vessel effects}} + \underbrace{\zeta_1(i)}_{\text{Catchability covariates}} \quad (3)$$

where $p_1(i)$ is the predictor for observation i, arising for category c_i at location s_i and time t_i. Similarly, the second linear predictor $p_2(i)$ represents positive catch rates in a delta model, where all variables and parameters are defined similarly except using different subscripts (Thorson and Barnett, 2017). The vessel effects are random effects represented the catches distribution of each commercial vessel in the database.

There are different user-controlled options for observation models for available sampling data. VAST distinguish between observation models for continuous-valued data (e.g., biomass, or numbers standardized to a fixed area), and observation models for count data (e.g., numbers treating area-swept as an offset). If using an observation model with continuous support (e.g., a log-normal, gamma distribution,…), then data b_i can be any non-negative real number, $b_i \in \mathcal{R}$ and $b_i \geq 0$. The VAST model implemented in this paper is the alternative "Poisson-link

delta-model" using log-link function (ObsModel[2]=1) in the R VAST packages) and gamma distribution.

ObsModel[2] = 1 corresponds to a "Poisson-link" delta-model that approximates a Tweedie distribution:

$$r_1(i) = 1 - \exp\left(-a_i \times \exp\left(p_1(i)\right)\right) \quad (4)$$

where $r_1(i)$ is the predictor encounter probability and $1 - \exp\left(-a_i \times \exp\left(p_1(i)\right)\right)$ is a complementary log-log link of $p_1(i) + \log(a_i)$, and:

$$r_2(i) = \frac{a_i \times \exp(p_1(i))}{r_1(i)} \times \exp(p_2(i)) \quad (5)$$

where $r_2(i)$ is the predicted biomass given that the species is encountered.

In that case, the expectation for sampling data is:

$$\mathbb{E}(B_i) = r_1(i) \times r_2(i) \quad (6)$$

VAST calculates the probability of these data as:

$$\Pr(b_i = B) = \begin{cases} 1 - r_1(i) & \text{if } B = 0 \\ r_1(i) \times g\{B \mid r_2(i), \sigma_m^2(c)\} & \text{if } B > 0 \end{cases} \quad (7)$$

where $g\{B \mid r_2(i), \sigma_m^2(c)\}$ is the probability density function used for positive catch rates.

the product of $r_1(i)$ and $r_2(i)$ is predicted biomass-density $d(g, c, t)$ at every extrapolation-grid cell g, category c, and time t. By default, density is used to predict total abundance for the entire domain (or a subset of the domain) for a given species:

$$I(c, t) = \sum_{x=1}^{n_x} (a(g) \times d(g, c, t)) \quad (8)$$

where $a(g)$ is the area associated with extrapolation-grid cell g and n_x the number of knots. To apply VAST for estimating BET tuna annual and seasonal standardized CPUE, we used a 55 km x 55 km grid cell aggregated in 100 knots (**Figure 1** and **2**). We estimated a yearly-basis and quarterly-basis models.

We examined four catchability covariates that may affect variation in catchability or detectability variation of BET schools: fishing_country, Is_fishing_own_fad, storage_capacity and (dFADs) density (See **Table 1** for more details). We test numerous models from the null model with no catchability covariates to the full model. The best model, based on AIC criterion, was the delta model with Is_fishing_own_fad (followed dFADs) and (dFADs) density as catchability covariate for the encounter probability component and Is_fishing_own_fad, fishing_country and (dFADs) density as catchability covariates for the catch rate of positive sets component.

Binomial component = ~ Is_fishing_own_fad+bs(log(density+2), degree=2, intercept=FALSE)

Catch rate component = ~ fishing_country+Is_fishing_own_fad+ bs(log(density+2), degree=2, intercept=FALSE).

bs(log(density+2), degree=2, intercept=FALSE) is a basis-spline with 2 degrees of freedom to model a nonlinear effect of log-transformed dFADs density

3. Results and discussion

In this paper, we used VAST to get a standardized CPUE which enables to account for an interactive relationship between space and time. The results of the GLMM approach are provided for the sake of continuity and to evaluate differences in the output derived to the modelling approach applied.

Standardized and nominal CPUEs are presented by year-quarter as well as by year (**Figure 3, 4, 5** and **6**, and **Table 4** and **5**). The recent version of VAST package allow probability integrate transform (PIT) residuals for delta-models, using DHARMa for plotting tools. The DHARMa-style residuals are then used to assess if model fit to the data. DHARMa-stlye residuals take advantage of this approach by defining the residuals based on where the observations fall in the distribution of simulated samples (Dunn and Smyth, 1996). In addition to accounting for the random effects, another advantage of this approach is that it allows the entire model structure, both components of the delta model, to be evaluated using a quantile-quantile (QQ) plot of the uniformly distributed model residuals.

The models appear to fit the data well (**Figure 8, 9, 10** and **11**) without indicating non-uniformity. Visualizing the residuals spatially and temporally, we see evidence that the model indicates a better fit to the data.

The influence plot shows that there seems to be a problem for the last two years (2020 and 2021) (**Figure 13**). We feel the changed in the standardized CPUE may be tainted by the fact that we do not have data for the two fleets.

Table 1. Candidate variables for the CPUE standardization models.

Variable (in the model)	**description**
BET	Capture of BET per positive set
year	Year at which the fishing set took place
yyqq	A quarter of the year at which the fishing set took place
area	5x5-degree grid cells where SKJ were fished for at least 150 sets.
numbat	Unique vessel identifier.
fishing_country	Fleet country: France and Spain
Is_fishing_own_fad	TRUE if the dFAD where the set takes place is owned by the vessel's company or FALSE otherwise.
storage_capacity	Vessel storage capacity in m
density	dFADs monthly average density in a 1x1-degree grid

Table 2. Analysis of Deviance Table [GLMM Lognormal for the catch rate component]

Variable	Variable	Deviance	Resid..Df	Resid..Dev	F	Pr..F.	Dev..Exp
NULL	NA	NA	42075	51003	NA	NA	NA
yyqq	47	5392	42028	45611	129	0	10.57 %
area	26	2271	42002	43340	98	0	4.45 %
fleet_country	1	655	42001	42685	736	0	1.28 %
storage_capacity	3	123	41998	42561	46	0	0.24 %
density	3	61	41995	42500	23	0	0.12 %
numbat	28	427	41967	42073	17	0	0.84 %
Is_fishing_own_fad	1	102	41966	41971	115	0	0.2 %
yyqq:fleet_country	914	5415	41052	36556	7	0	10.62 %

The proportion of deviance explained by the best model of this component was 28.33%.

Table 3. Analysis of Deviance Table [GLMM binomial for the binomial component]

Variable	Df	Deviance	Resid..Df	Resid..Dev	Pr..Chi.	Dev..Exp
NULL	NA	NA	44149	16734	NA	NA
yyqq	47	394	44102	16340	0.000	2.36 %
area	26	241	44076	16098	0.000	1.44 %
fleet_country	1	796	44075	15302	0.000	4.76 %
storage_capacity	3	48	44072	15254	0.000	0.29 %
density	3	1	44069	15253	0.773	0.01 %
numbat	29	293	44040	14960	0.000	1.75 %
Is_fishing_own_fad	1	46	44039	14914	0.000	0.27 %
yyqq:fleet_country	39	179	44000	14735	0.000	1.07 %

The proportion of deviance explained by the best model for this component was 11.91%.

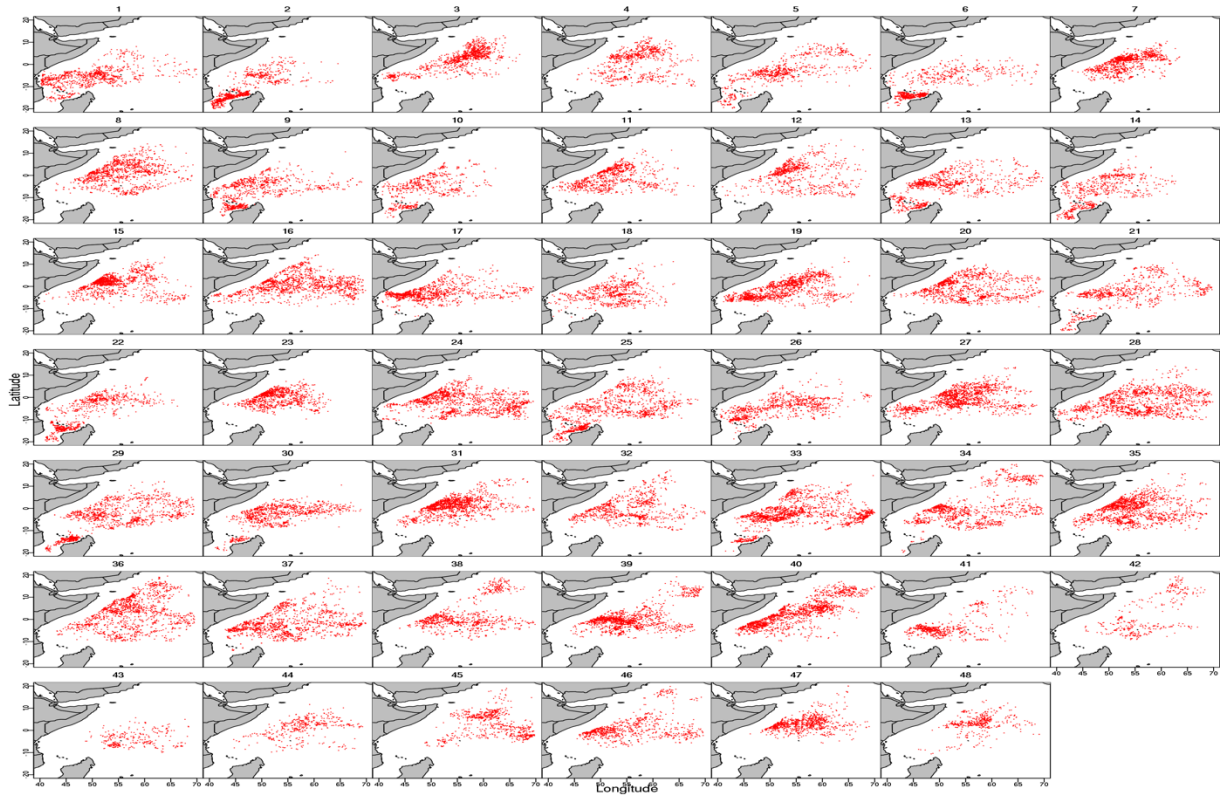

Figure 1: Spatial distribution of the fishing operations made on drifting FADs by the European purse seiner (Q1 2010 – Q4 2021) in the Indian Ocean (after data cleaning).

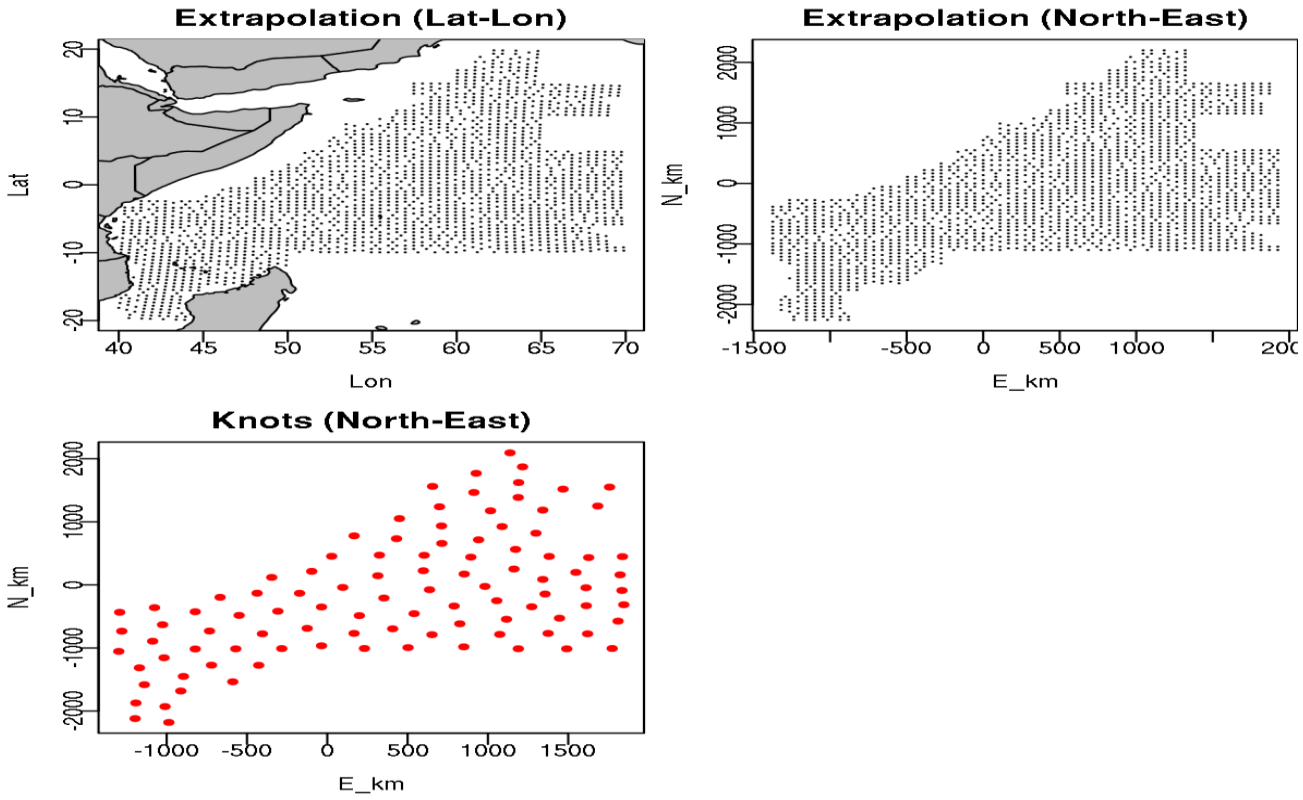

Figure 2 : Spatial distribution of the extrapolation grid cell (55km x 55km, black points) aggregated in 100 knots (red points).

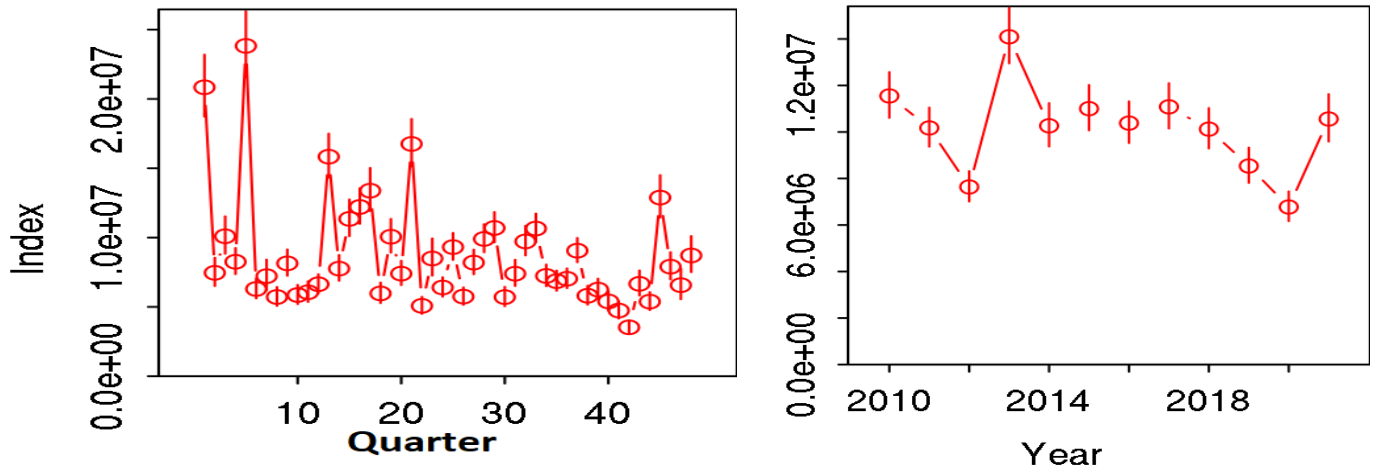

Figure 3: Standardized CPUE for spatio-temporal model (VAST results)

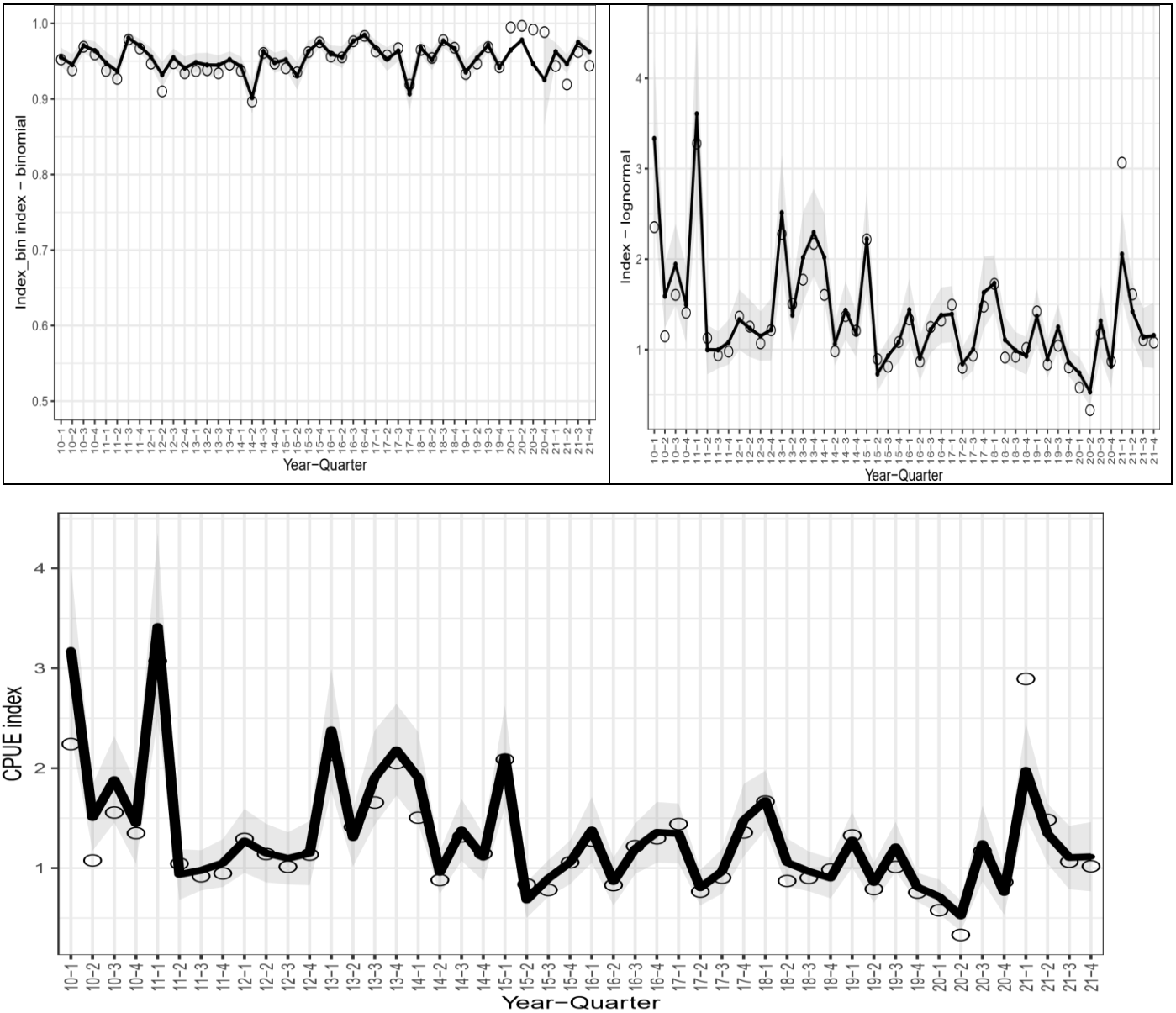

Figure 4: GLMM results (topleft: binomial GLMM; topright: log-normal GLMM and bottom: delta lognormal).

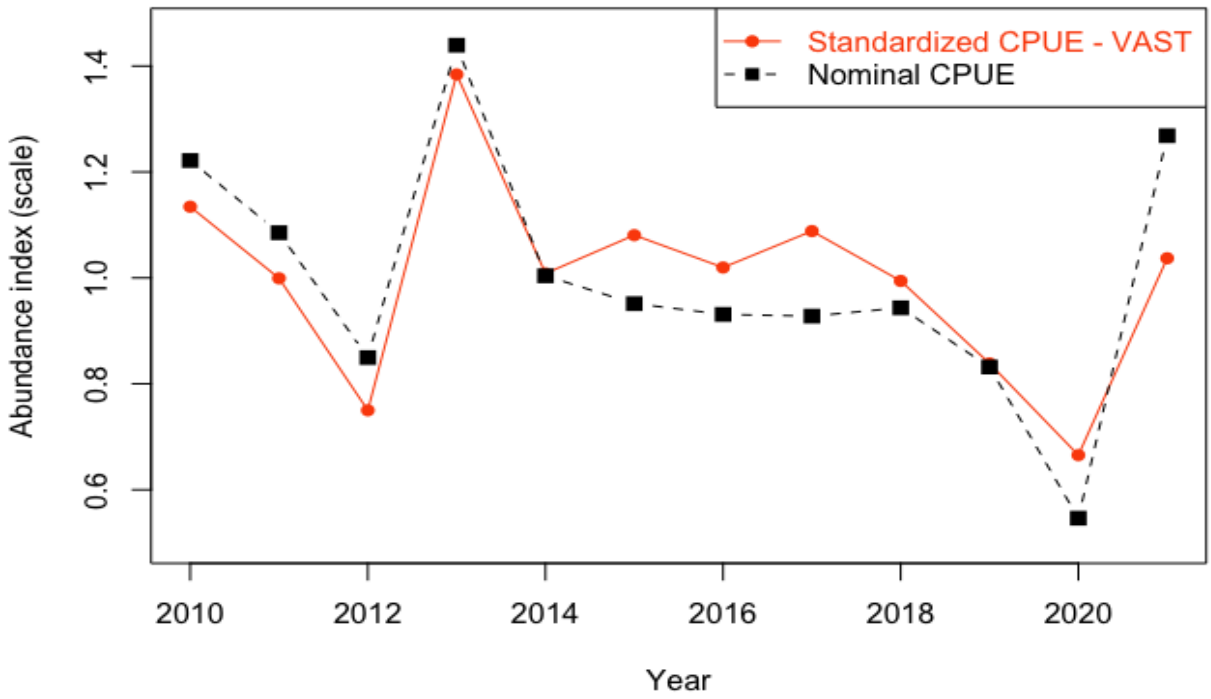

Figure 5: Relative standardized CPUE (scaled) (red line for the VAST model) compared to nominal CPUE (black). Time series on a year basis.

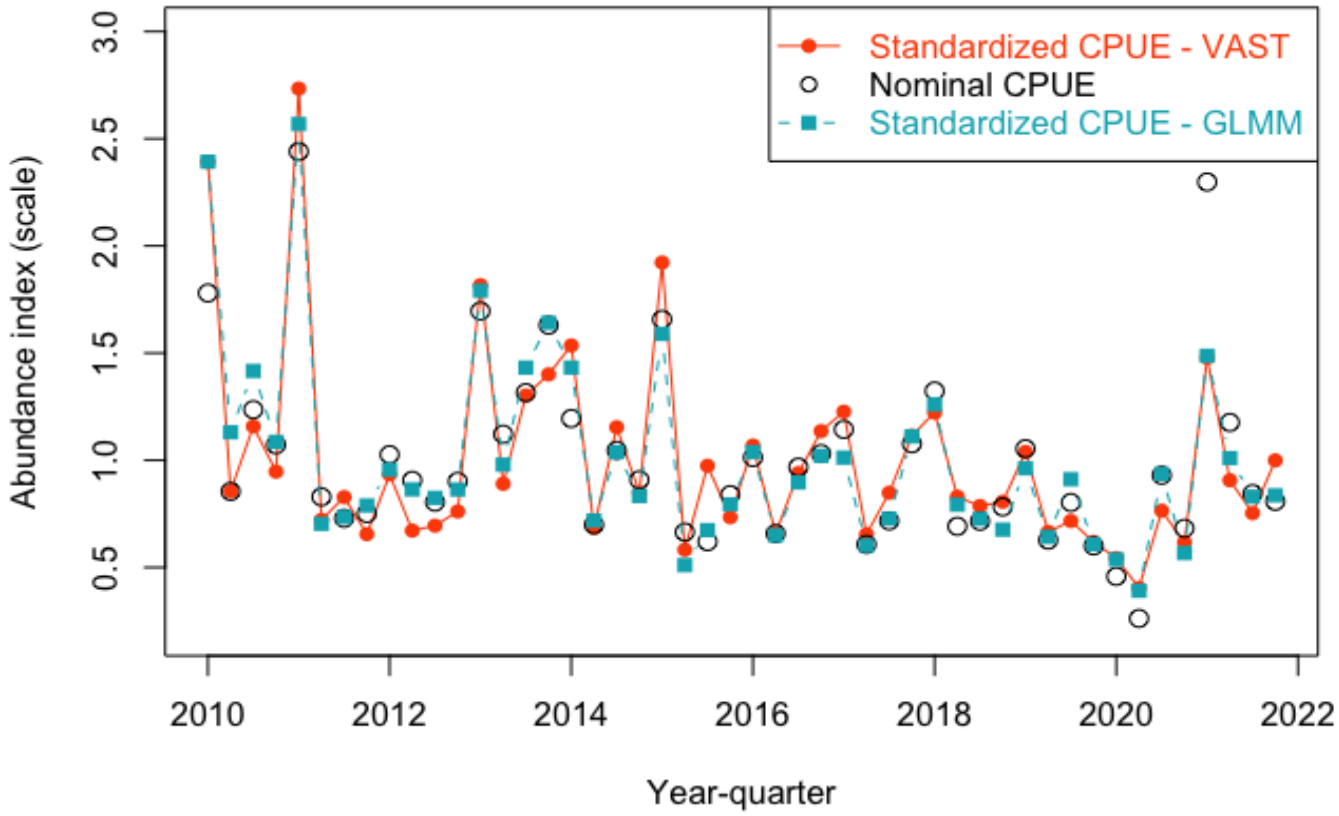

Figure 6: Relative standardized CPUE (scaled) (red for the VAST model and blue for the GLMM model), and compared to nominal CPUE (black). Time series on a quarterly basis.

Residuals vs Fitted

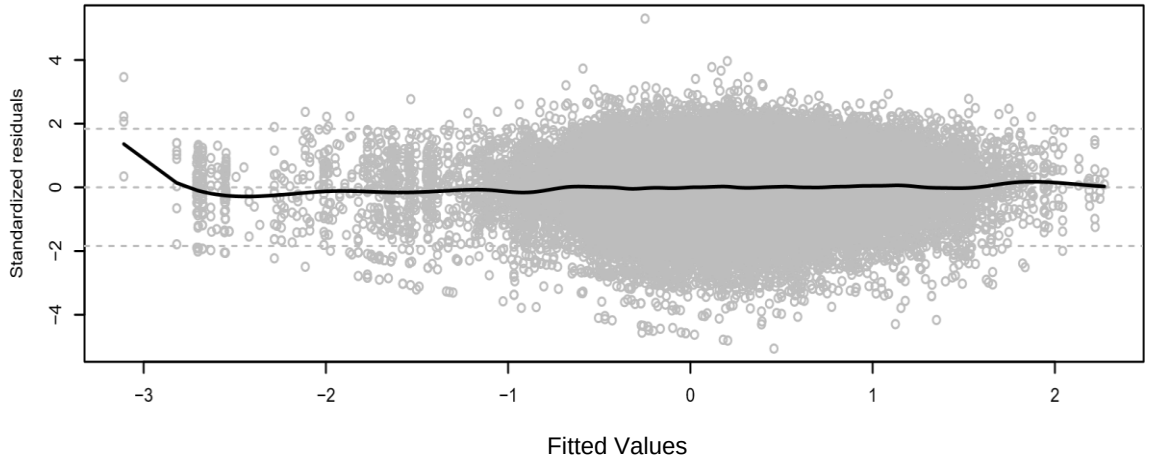

Normal Q−Q Plot

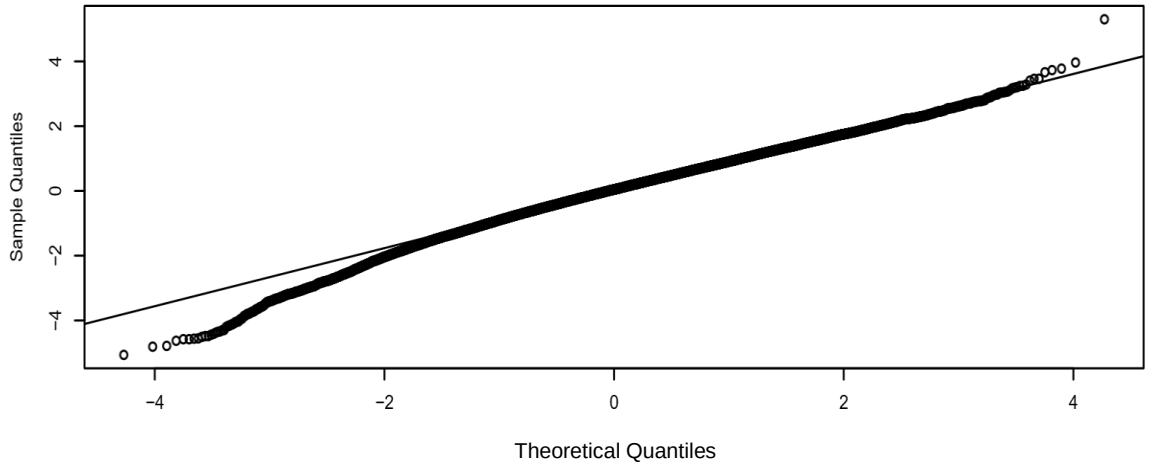

Histogram residuals

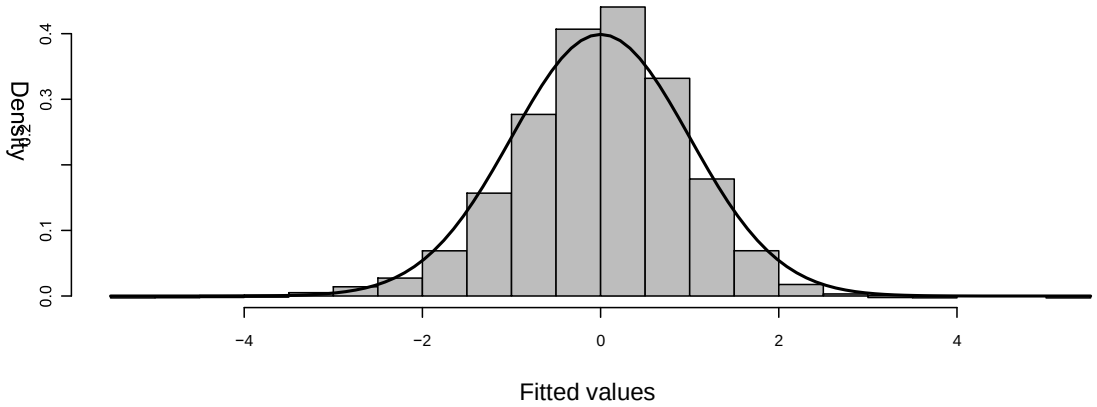

Figure 7. Diagnostics of the lognormal-GLMM analysis (catch rate): residuals vs fitted, Normal Q-Q plot and frequency distributions of the residuals.

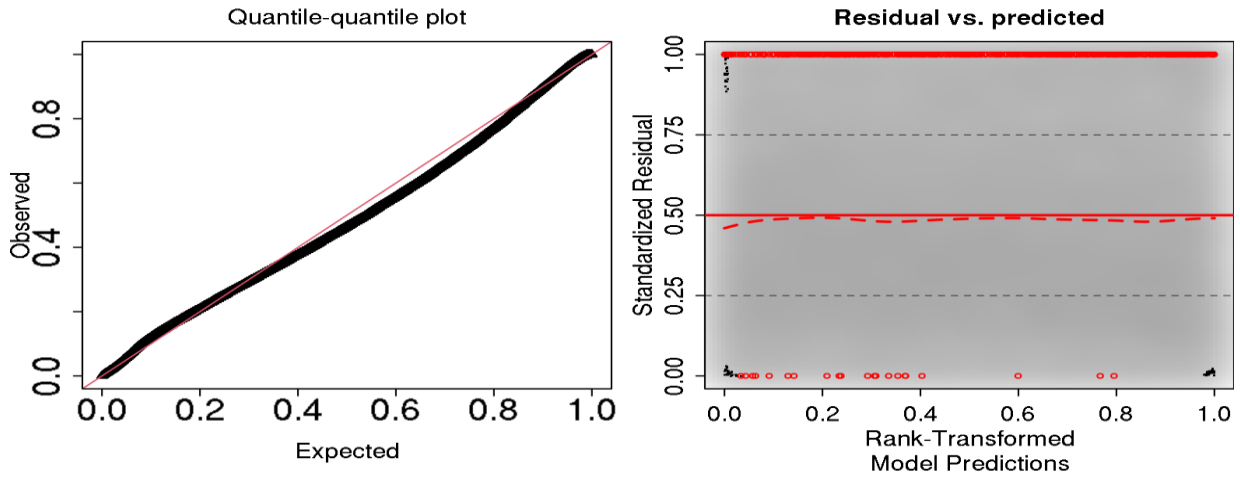

Figure 8: Uniform Quantile-Quantile (QQ) (left panel) and residuals against the predicted value plot of the DHARMa calculated residuals for the annual VAST model (right panel).

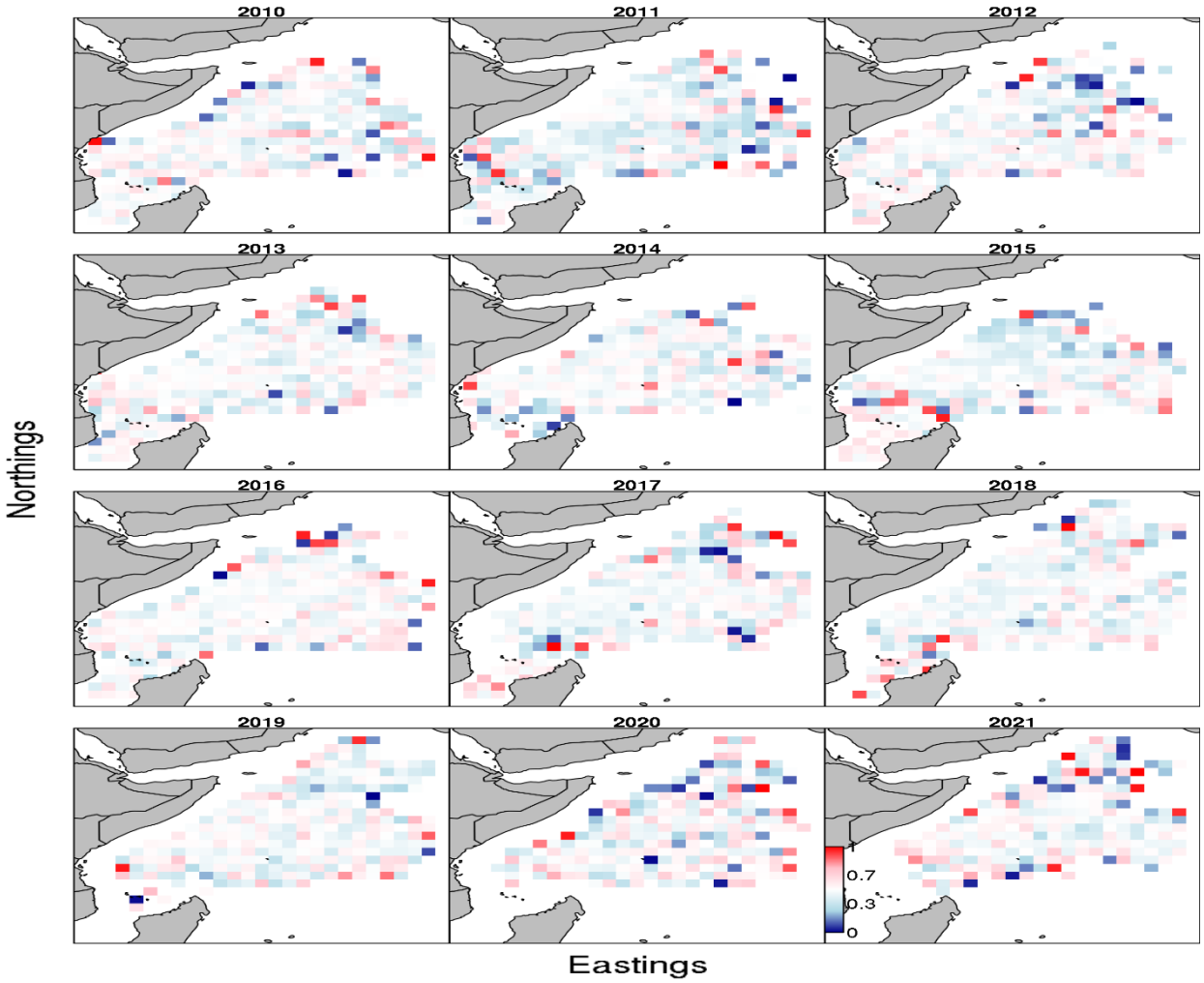

Figure 9: Spatiotemporal aggregated quantile residuals from the VAST model. Time series on a year basis

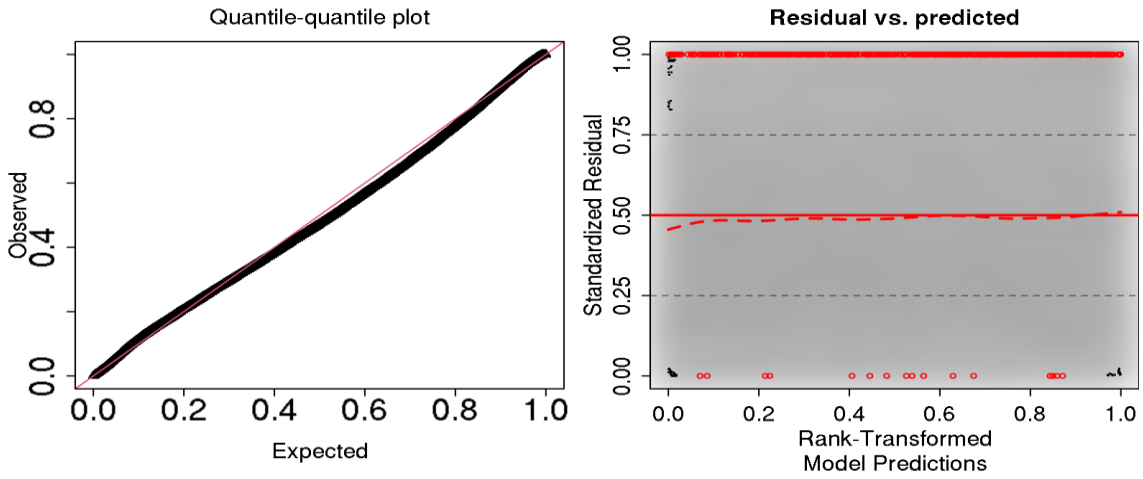

Figure 10: Uniform Quantile-Quantile (QQ) (left panel) and residuals against the predicted value plot of the DHARMa calculated residuals for the quarterly model (right panel).

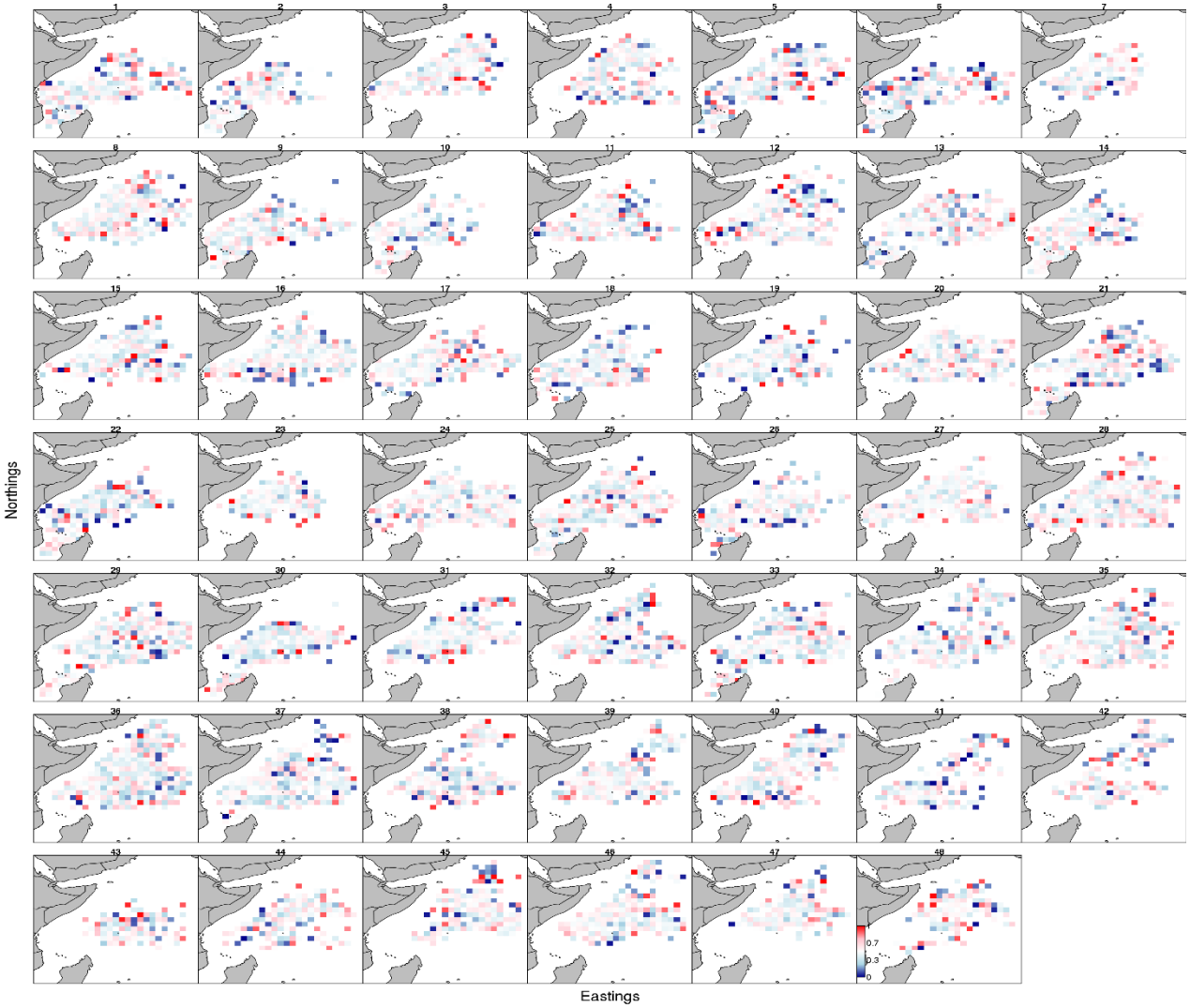

Figure 11: Spatiotemporal aggregated quantile residuals from the VAST model. Time series on a quarterly basis.

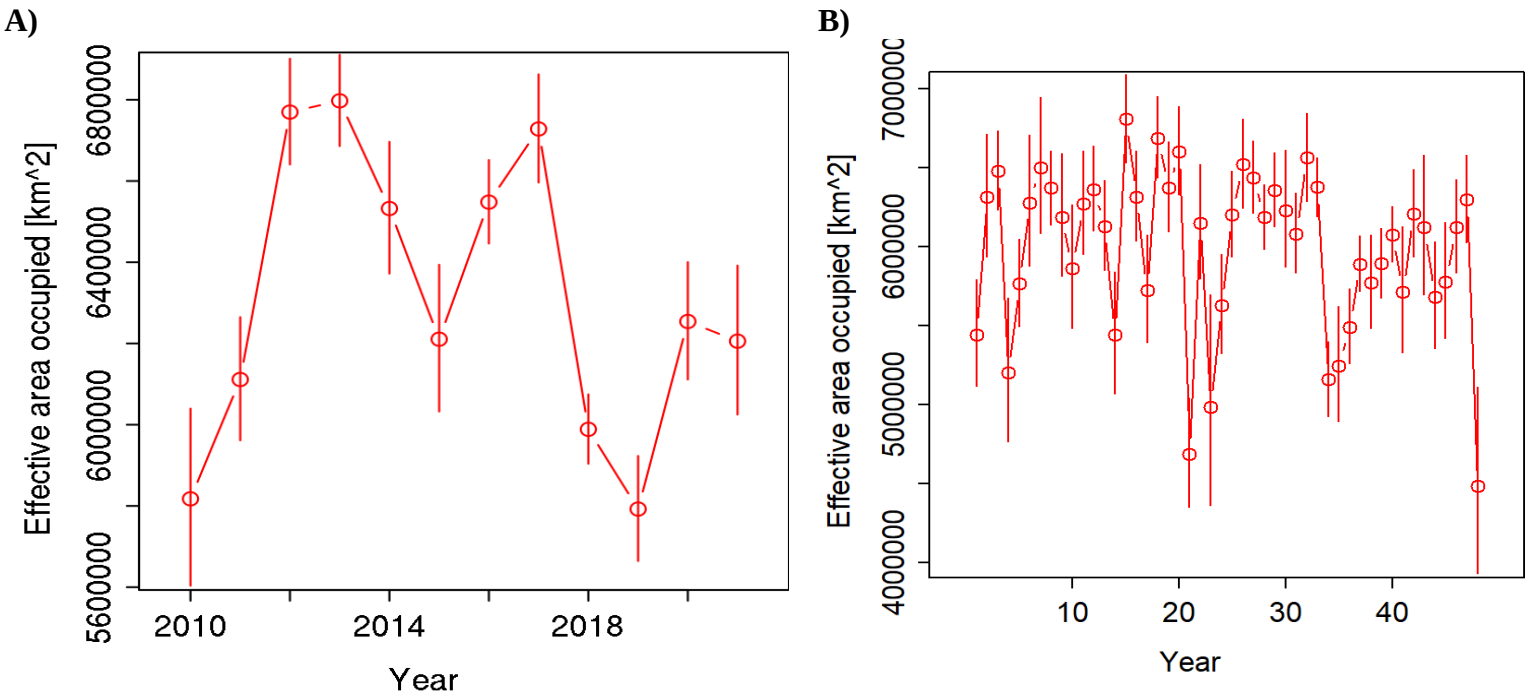

Figure 12: Estimated effective area occupied [which measures the area (in units square km) required to contain a population given its average population density (kg km−2)] of BET caught by the European purse seiner for fishing operations made on dFADs in indian ocean. Each panel shows the estimate (circle) and confidence interval (±1 s.e.; y-axis) against time (x-axis). Figure A is in an annual basis and figure B (from Q1-2010 to Q4-2021) in a quarterly basis. For the modelling, an extrapolation grid of 55km x 55km (~0.5-degree square) was considered for the population density estimate.

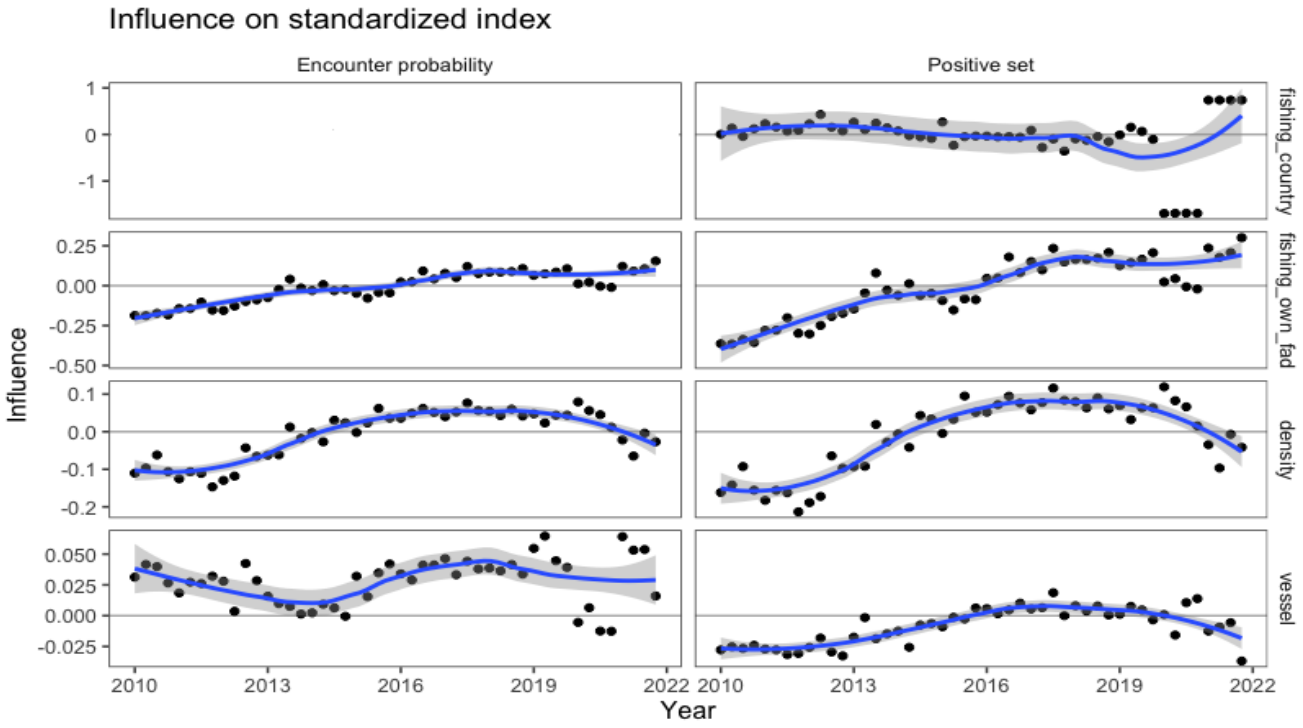

Figure 13: Influence plot (VAST model) for each covariate and each model component, showing the effective correction in the standardized CPUE as a result of a change over time of some associated factors. Time series are on a quarterly basis.

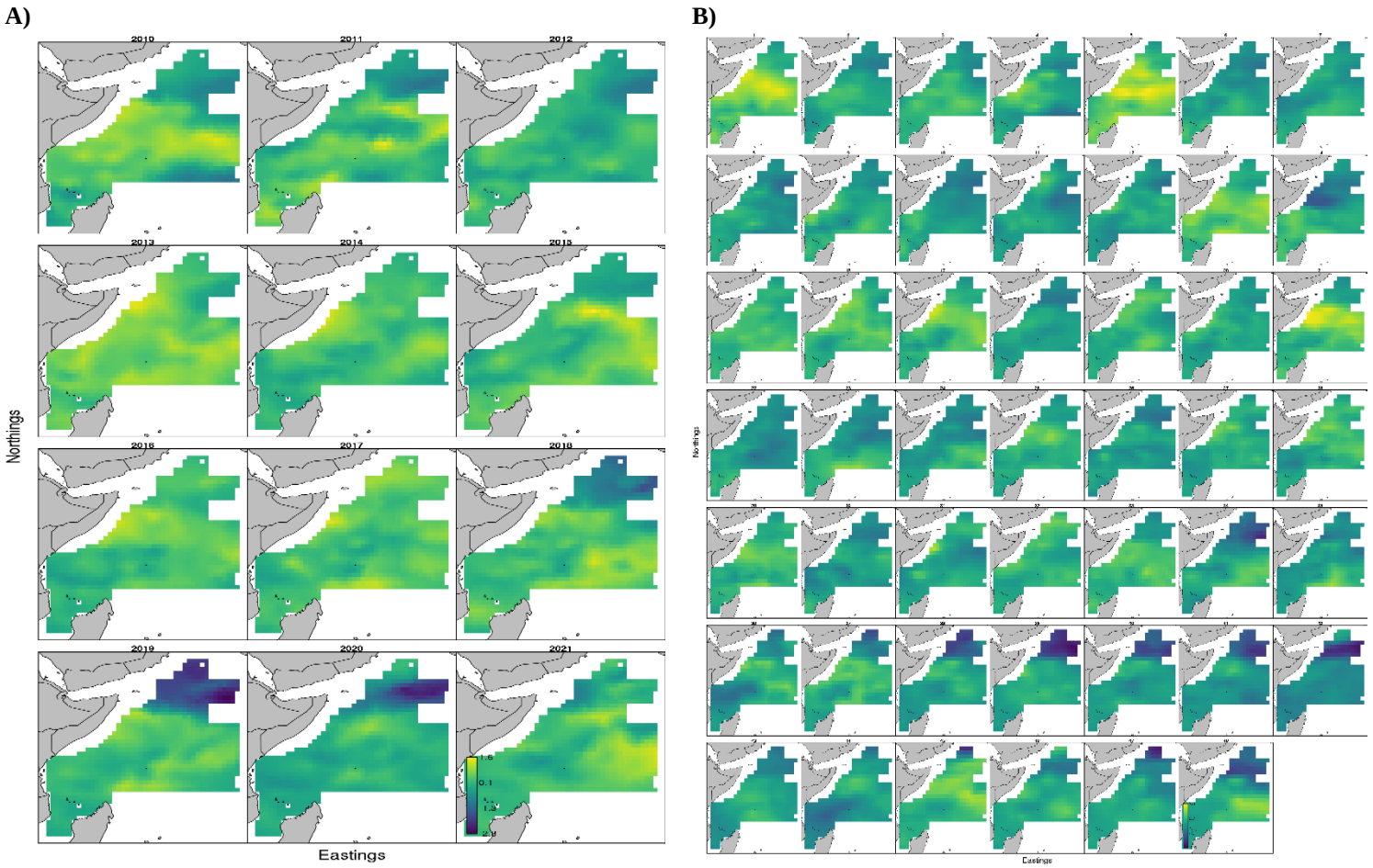

Figure 14: Predicted estimates of spatiotemporal relative catch rate per positive dFAD set. Figure A is on a yearly basis and figure B on a quarterly basis.

Table 4. Standardized CPUE (VAST) vs Nominal CPUE per year

Year	Results from the VAST model		
	Standardized CPUE (scaled)	Nominal CPUE (scaled)	SE (log estimated)
2010	1.1344165	1.2215807	0.08523399
2011	0.9992612	1.0853140	0.08278903
2012	0.7500243	0.8496061	0.08556966
2013	1.3841212	1.4392343	0.08469594
2014	1.0083260	1.0039907	0.09105005
2015	1.0806511	0.9514046	0.08871008
2016	1.0196105	0.9310314	0.08631635
2017	1.0883718	0.9278100	0.08817954
2018	0.9942481	0.9435132	0.08595264
2019	0.8385044	0.8317681	0.08900572
2020	0.6654051	0.5463094	0.09467189
2021	1.0370598	1.2684376	0.09667843

Table 5. Standardized CPUE (VAST and GLMM) vs Nominal CPUE per quarter

Year-quarter	Standardized CPUE VAST (scaled)	Standardized CPUE GLMM (scale)	Nominal CPUE (scaled)	SE –VAST Model (log estimated)
01_2010	2.3912617	2.3926357	1.7800725	0.10718255
02_2010	0.8554831	1.1309412	0.8546890	0.13669376
03_2010	1.1580918	1.4164945	1.2359629	0.13357479
04_2010	0.9470250	1.0858538	1.0723328	0.11417947
01_2011	2.7337084	2.5684764	2.4401529	0.09977252
02_2011	0.7219564	0.7033628	0.8292707	0.11460051
03_2011	0.8280859	0.7349239	0.7291863	0.15335909
04_2011	0.6555184	0.7890287	0.7514273	0.11926712
01_2012	0.9338857	0.9558520	1.0262622	0.11694288
02_2012	0.6718561	0.8641743	0.9063198	0.11850700
03_2012	0.6949066	0.8243472	0.8046468	0.12316755
04_2012	0.7611949	0.8634229	0.9015539	0.10348782
01_2013	1.8166480	1.7907195	1.6958745	0.10014078
02_2013	0.8902765	0.9798986	1.1215807	0.11967784
03_2013	1.3020443	1.4322750	1.3153949	0.11650557
04_2013	1.4004921	1.6411798	1.6299459	0.10487773
01_2014	1.5354059	1.4322750	1.1946582	0.11581048
02_2014	0.6849574	0.7191433	0.6990021	0.12421595
03_2014	1.1541753	1.0377607	1.0461202	0.12072047
04_2014	0.8488299	0.8333646	0.9087028	0.11881406
01_2015	1.9223790	1.5893293	1.6569528	0.10231040
02_2015	0.5822623	0.5109900	0.6648463	0.12133278
03_2015	0.9741689	0.6740560	0.6203644	0.15760296
04_2015	0.7342370	0.7942889	0.8395969	0.10936256
01_2016	1.0685326	1.0377607	1.0127588	0.10474172
02_2016	0.6587914	0.6500094	0.6584918	0.10981438
03_2016	0.9401538	0.8964869	0.9682768	0.10837934
04_2016	1.1359227	1.0204772	1.0310281	0.10242568
01_2017	1.2265567	1.0122112	1.1438217	0.10233248
02_2017	0.6547465	0.6026677	0.6076553	0.12277562
03_2017	0.8482285	0.7274094	0.7172715	0.12793560
04_2017	1.1152554	1.1114033	1.0770987	0.10977826
01_2018	1.2218763	1.2601916	1.3233381	0.09707752
02_2018	0.8298591	0.7927860	0.6918532	0.10821409
03_2018	0.7863820	0.7266579	0.7156829	0.10615672
04_2018	0.8065244	0.6763104	0.7824058	0.10160661
01_2019	1.0387387	0.9626151	1.0540634	0.09695608
02_2019	0.6658895	0.6424948	0.6275133	0.11768695
03_2019	0.7170781	0.9115161	0.8030581	0.11895265
04_2019	0.6188398	0.6079279	0.6005064	0.12958323
01_2020	0.5437211	0.5372910	0.4583230	0.13076626
02_2020	0.4045084	0.3915085	0.2621258	0.13371472
03_2020	0.7646108	0.9363141	0.9301494	0.13526918
04_2020	0.6172200	0.5673492	0.6823214	0.12069898
01_2021	1.4782711	1.4871313	2.2979695	0.11868032
02_2021	0.9066583	1.0099568	1.1763888	0.12441402
03_2021	0.7534477	0.8303588	0.8443628	0.16820648
04_2021	0.9993368	0.8363705	0.8086184	0.14906678

References

Chassot, E. et al. (2012) ‘The tuna fishery and piracy. In: Norchi CH, Proutière-Maulion G (eds) Piracy in comparative perspective: Problems, strategies, law.’, Editions A. Pedone & Hart Publishing, Oxford, United Kingdom, pp. 52–72.

Dunn, P. K. and Smyth, G. K. (1996) ‘Randomized Quantile Residuals’, Journal of Computational and Graphical Statistics, 5(3), pp. 236–244. doi: 10.1080/10618600.1996.10474708.

Grüss, A. et al. (2019) ‘Evaluation of the impacts of different treatments of spatio-temporal variation in catch-per-unit-effort standardization models’, Fisheries Research. doi: 10.1016/j.fishres.2019.01.008.

Guillotreau, P. et al. (2012) ‘The economic impact of piracy on the EU purse-seine tuna fishery in the West Indian Ocean.’, International Workshop on “The impacts of piracy on fisheries in the Indian Ocean”, 28-29 February. European Bureau for Conservation & Development, Mahé, Republic of Seychelles.

ICCAT (2016) ‘Recommendation by ICCAT on a multi-anual conservation and management programme for tropical tunas. Rec 16-01’.

Okamoto, H. (2011) Preliminary analysis of the effect of the Piracy activity in the northwestern Indian Ocean on the CPUE trend of bigeye and yellowfin.

Pallarés, P. and Hallier, J. P. (1997) ‘Analyse du schéma d’échantillonnage multispécifique des thonidés tropicaux’, Rapport scientifique. IEO/ORSTOM, Programme, 95, p. 37.

Thorson, J. T. et al. (2015) ‘Geostatistical delta-generalized linear mixed models improve precision for estimated abundance indices for West Coast groundfishes’, ICES Journal of Marine Science, 72(5), pp. 1297–1310. doi: 10.1093/icesjms/fsu243.

Thorson, J. T. (2019) ‘Guidance for decisions using the Vector Autoregressive Spatio-Temporal (VAST) package in stock, ecosystem, habitat and climate assessments’, Fisheries Research, 210, pp. 143–161. doi: 10.1016/j.fishres.2018.10.013.

Thorson, J. T. and Barnett, L. A. K. (2017) ‘Comparing estimates of abundance trends and distribution shifts using single-and multispecies models of fishes and biogenic habitat’, ICES Journal of Marine Science, 74(5), pp. 1311–1321.

Wain, G. et al. (2020) ‘Quantifying the increase in fishing efficiency due to the use of drifting FADs equipped with echosounders in tropical tuna purse seine fisheries’, ICES Journal of Marine Science, 78(1), pp. 235–245. doi: 10.1093/icesjms/fsaa216.